



JAN SZANTYR, Prof., D.Sc., N.A.
Polish Academy of Sciences
Institute of Fluid Flow Machinery
Gdańsk

Design and analysis of surface piercing propellers

SUMMARY

The surface piercing propellers are promising propulsors for high speed craft, already proven by many full scale applications on small racing and sports boats. This paper presents newly developed theoretical procedures for design and hydrodynamic/strength analysis of such propellers. The design procedure is based on the lifting line theory while the analysis is performed by means of the lifting surface/finite element method.

These procedures are confronted with the results of a series of model experiments by which surface piercing propellers were thoroughly tested in single and twin screw configurations. This confrontation demonstrates correctness of the basic theory and practical value of the design and analysis procedures.

GENERAL IDEA OF SURFACE PIERCING PROPELLERS

The rapidly growing popularity of civilian and military fast craft has stimulated increased interest in surface piercing propellers (SPP) as the propulsors which are particularly suited for the craft. Up to now such propellers have been used mostly for very small pleasure boats and their design was based simply on trial and error procedure with full scale prototypes. The complicated character of physical phenomena accompanying the operation of SPP has precluded development of theoretical design procedures of acceptable accuracy. Such methods are in great demand now, along with the growing size and power of new SPP applications. They are partly substituted by the results of systematic model experiments which have been conducted in several model basins recently [6] and which may be applied to preliminary design.

The most characteristic feature of the surface piercing propellers is their operation with hub located above water. Thrust is generated only by the outward sections of the blades which pass through the phases of water entry, submerged operation and water exit. In the second phase cavitation or full ventilation is present on the suction side, depending on the propeller loading. Full ventilation protects the blades against cavitation erosion. Elevation of the hub above water reduces friction losses and together with immersion of the outer blade sections only it results in a relatively high efficiency of SPP. On the other hand the partial submergence of the propeller leads to generation of high transverse forces both in vertical and horizontal directions. The forces affect yaw and trim angles of the boat, thus their values become important design parameters. Another typical feature of SPPs is their high loading at low speed, resulting from an increased submergence. This may prevent developing full engine power in this condition, leading to difficulties in passing through the resistance hump. This problem is often solved by introducing the controllable pitch or by adding the controllable flaps in front of the propeller. Highly variable hydrodynamic loading of the blades during every revolution results in serious strength, vibration and hydroelasticity problems which should be properly addressed during the development of the design.

Full design process of the surface piercing propellers requires at least two computation methods, namely: a design method supplying the necessary propeller geometry which fulfils the design requirements, e.g. [7], and an analysis method, e.g. [1,3], which makes calculating the variable loads, stress distributions and deformations of the designed blade possible. The first method is used, according to the generally accepted design philosophy, for initial estimation of the propeller geometry while the other is employed for optimization of the geometry. Consequently the first method is based on the relatively simple lifting line model while the second makes use of the more sophisticated lifting surface/finite element models. Both methods together form a unique system of programs for design and analysis of the surface piercing propellers.

MODEL EXPERIMENTS

The purpose of model experiments with surface piercing propellers was twofold: firstly to provide insight into the complicated flow phenomena associated with their operation, secondly to supply results of measurement suitable for the initial experimental verification of the numerical procedures. A pair of left- and right-handed controllable pitch surface piercing propeller models were manufactured for the experiments, based on the data collected from the literature. A special experimental stand shown schematically in Fig. 1, was assembled in the model basin of the Ship Design and Research Centre (CTO), Gdańsk. The models were tested in single and twin

screw configurations. The varied parameters included: submergence, yaw and trim angles, direction of rotation (in twin screw configuration) and the advance coefficient. The measured quantities were: mean thrust and torque, rotational and advance speed of the propeller, mean transverse forces on the shaft and time-dependent bending moments on a single blade. Altogether 16 operating conditions were tested for a single propeller and 24 conditions for the twin-screw configuration. Complete results of the model experiments may be found in [2,4].

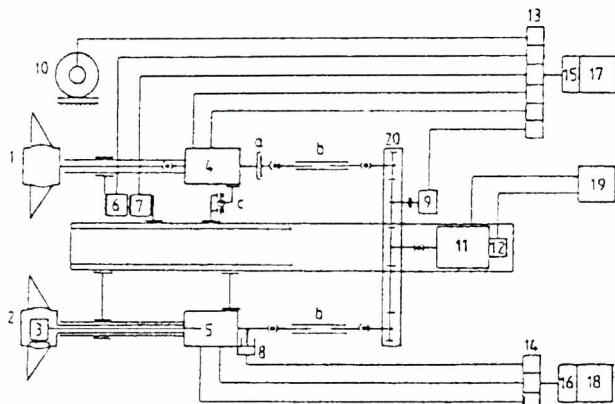


Fig.1. Scheme of the test stand for experiments with surface piercing propellers

- | | |
|-------------------------------------|----------------------------------|
| 1 - right-hand propeller model | 11 - asynchronous electromotor |
| 2 - left-hand propeller model | 12 - electromotor speed encoder |
| 3 - two-component blade dynamometer | 13,14 - electronic bridges |
| 4 - shaft dynamometer | 15,16 - electronic bridges |
| 5 - slipping signal transmission | 17,18 - PCs |
| 6,7 - transverse force dynamometer | 19 - electromotor control system |
| 8 - photoelectric encoder | 20 - multi-input/output gear |
| 9 - tachogenerator | a - adjustable coupling |
| 10 - carriage speed measuring wheel | b - telescopic shafts |
| | c - Cardane mounting |

THEORETICAL MODEL FOR DESIGN

The typical geometric/kinematic/dynamic situation of a surface piercing propeller is shown in Fig.2. In most cases the input data for design consist of :

- | | |
|---|-----------------------------------|
| propeller diameter - D | hub diameter - d |
| number of blades - z | blade tip submergence - H_T |
| shaft inclination in both planes : | |
| vertical - the trim angle ξ | horizontal - the yaw angle ψ |
| number of propeller revolutions per second - n | |
| required propelling force (in direction of ship motion) - T_N | |

The design calculation results should include the following information :

- | | |
|---|-----------------------|
| mean shaft transverse forces (vertical - F_z , horizontal - F_y) | detail blade geometry |
| required power absorption - N | |
| propulsive efficiency - η_p | |

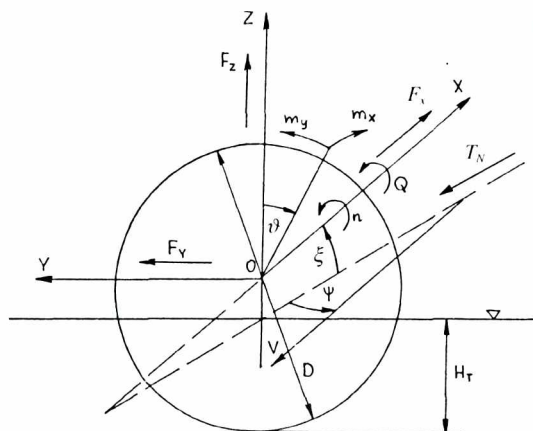


Fig.2. Geometric, kinematic and dynamic parameters of a surface piercing propeller

The design calculation is performed by means of a special version of the lifting line model shown schematically in Fig.3 and described in greater detail in [5]. The most characteristic feature of this model comes from the fact that the propeller disc and the propeller slipstream are cut by the free surface. This has two consequences: the free vortex surfaces behind propeller are discontinuous and a completely imaginary vortex system must be added above free surface in order to fulfil the boundary condition on this surface. The imaginary vortex system is a mirror reflection of the true vortex system and it takes part in the calculation of the induced velocity. Of course in reality the free surface in the vicinity of the operating propeller is not flat, so the scheme presented in Fig.3 may be regarded only as a simplified model.

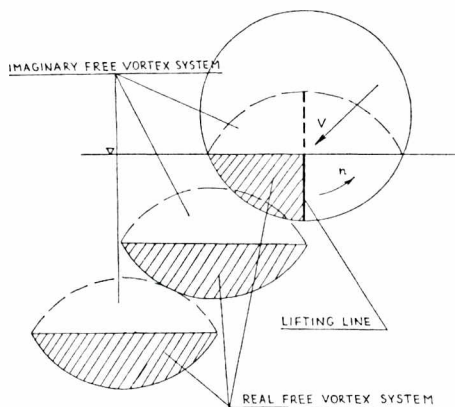


Fig.3. Scheme of the lifting line model for design of surface piercing propellers

The design calculation starts with the initial estimation of the blade area ratio, blade pitch and pitch distribution of the free vortex lines. This is done by means of approximate empirical formulae. The free vortex system is formed corresponding to the „vertical down” position of one of the blades. Then the components of the induced velocity are calculated by using Biot-Savart formula. When they are known the pitch distribution of the free vortex system may be computed again. This should be in compliance with the initially assumed distribution. The discrepancy between the two is reduced to an acceptable level during an iterative process. When this is finished the components of the hydrodynamic force on the blade in vertical down position may be calculated according to the following formulae :

$$F_x = \frac{1}{2} \rho V^2 \int_{r_i}^1 c(r) [c_L \sin \beta_i - c_D \cos \beta_i] \frac{\cos^2(\beta_i - \beta)}{\sin^2 \beta} dr \quad (1)$$

$$F_y = \frac{1}{2} \rho V^2 \int_{r_i}^1 c(r) [c_L \cos \beta_i + c_D \sin \beta_i] \frac{\cos^2(\beta_i - \beta)}{\sin^2 \beta} dr \quad (2)$$

In order to obtain the propelling force the contributions from all blades with taking into account their immersion must be geometrically added and an appropriate time average value must be taken. It is assumed that the radial distribution of the hydrodynamic force remains the same on the blades in other positions but it is limited to the submerged portion of the blade only. This leads to the following formulae for the mean propelling force :

$$T_N = \frac{1}{2\pi} \left[\cos \xi \int_{\vartheta_1}^{\vartheta_2} F_x(\vartheta) d\vartheta - \sin \xi \int_{\vartheta_1}^{\vartheta_2} F_y(\vartheta) \sin \vartheta d\vartheta + \sin \psi \int_{\vartheta_1}^{\vartheta_2} F_y(\vartheta) \cos \vartheta d\vartheta \right] \quad (3)$$

The area of the propeller blades is automatically increased and the design calculation is repeated if the propelling force is lower than the design value. If this does not solve the problem and the limiting

blade area is reached the specified propeller immersion is increased automatically. If still the required propelling force can not be generated and the hub reaches water surface, the program stops and suggestion is made to the user about a necessary increase of the propeller diameter. The absorbed power coefficient and propulsive efficiency are computed, if the design value of the propelling force is obtained, according to the following formulae :

$$N = \pi \rho n V^2 \sum_{i=1}^z \int_{r_i}^1 [c_L \cos \beta_i + c_D \sin \beta_i] \frac{\cos^2(\beta_i - \beta)}{\sin^2 \beta} c(r) r dr \quad (4)$$

$$\eta_p = \frac{T_N V}{N} \quad (5)$$

Finally the detail geometry of the designed propeller is calculated and the standard drawing of the propeller is prepared, an example of which is given in Fig.4. A reconstruction of the tested SPP model by means of the design procedure was attempted in order to confront the design procedure with the experiments. The design point was defined by the advance coefficient $J = 1.0$ and thrust coefficient $k_T = 0.054$ taken from the experimental characteristics of the model. Propeller immersion was assumed equal to 0.4 without any yaw and with trim angle equal to 6.6° . The calculation should reproduce the actual model geometry as close as possible. The comparison of the actual model and design geometry is given in Tab.1. As may be observed the calculation has virtually reproduced the model geometry. This suggests that the theoretical model and the numerical procedure are essentially correct.

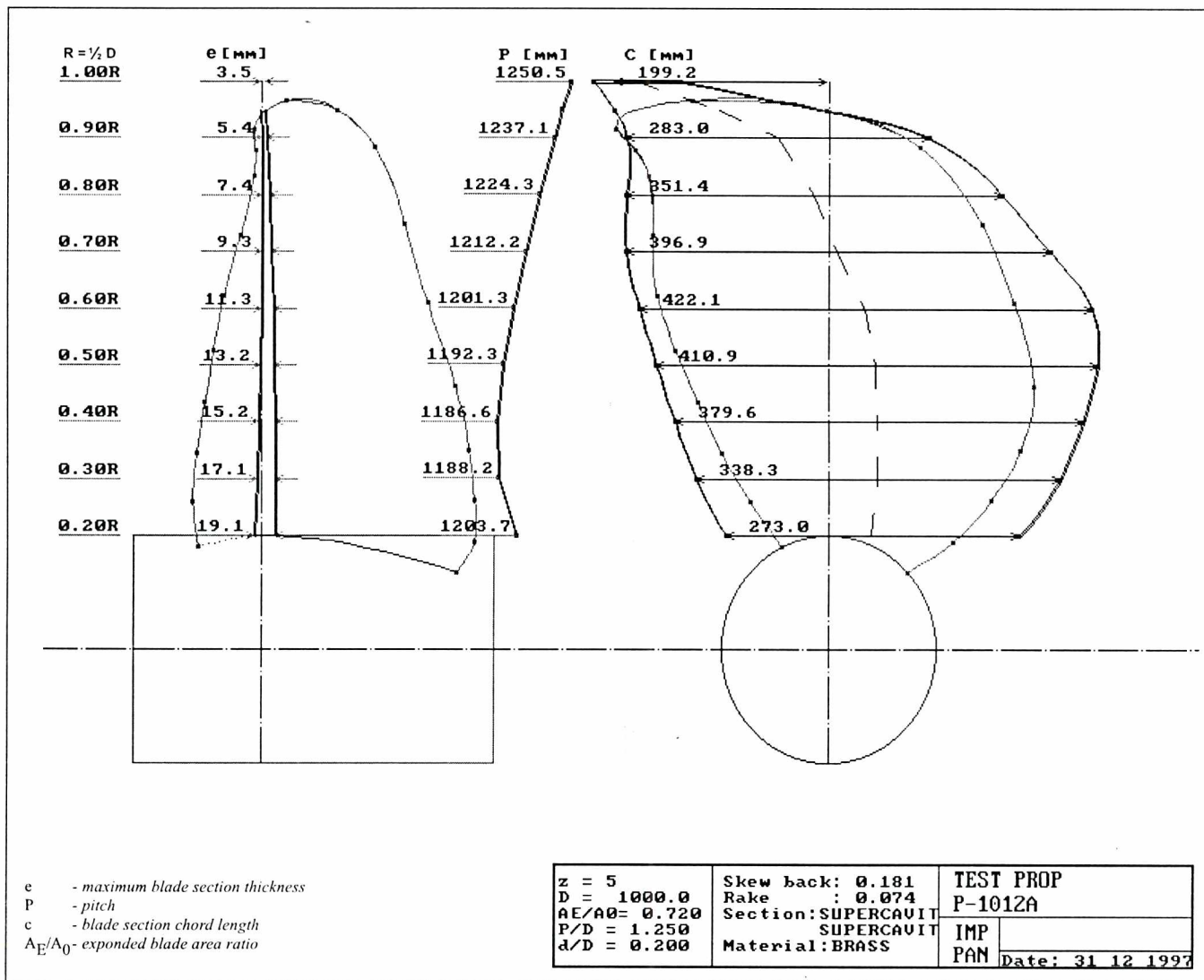


Fig.4. Drawing of the designed surface piercing propeller

Tab. Comparison of the tested and designed surface piercing propeller

z	MODEL			DESIGN		
	e	P/D	t/c	e	P/D	t/c
D[m]	0.220			1.0		
d[m]	0.075			0.341		
AE/A0	0.720			0.720		
r	e/D	P/D	t/c	e/D	P/D	t/c
0.35	0.2922	0.973	0.0346	0.3582	1.186	0.0331
0.40	0.3486	1.034	0.0293	0.3796	1.188	0.0299
0.50	0.3918	1.095	0.0291	0.4109	1.192	0.0293
0.60	0.4218	1.164	0.0275	0.4221	1.201	0.0276
0.70	0.4218	1.232	0.0260	0.3969	1.212	0.0262
0.80	0.3890	1.240	0.0245	0.3514	1.224	0.0250
0.90	0.3032	1.240	0.0229	0.2831	1.237	0.0232
0.95	0.2150	1.240	0.0224	0.1992	1.243	0.0226
1.00	0.1068	1.240	0.0212	0.0822	1.250	0.0214

THEORETICAL MODEL FOR HYDRODYNAMIC AND STRUCTURAL ANALYSIS

The purpose of the hydrodynamic and structural analysis of surface piercing propellers is to determine the time-dependent pressure distribution on the blades together with the resulting distribution of blade stresses and blade deformations. The first part of the analysis is based on the specially modified lifting surface theory while the second part is performed by the finite element method (FEM).

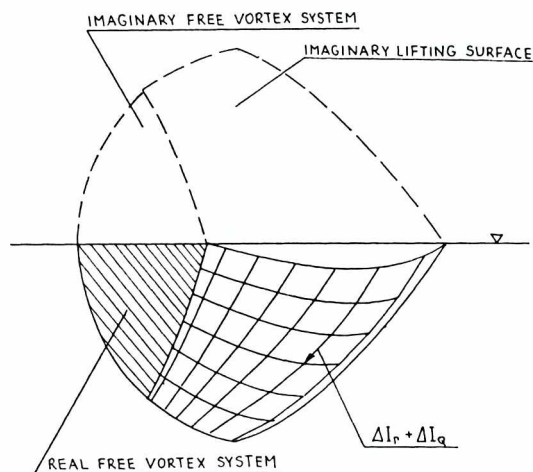


Fig.5. Lifting surface model for analysis of surface piercing propellers

The scheme of the lifting surface model is presented in Fig.5. More detail description of the model may be found in [5]. It is assumed that the hydrodynamic loading on the blade is modelled by the distribution of the discrete vortex elements ΔI_r while the thickness of the blade together with the thickness of the ventilating bubble on the suction side is modelled by the discrete source/sink elements ΔI_q . Determination of the unknown intensity of the vortices Γ and sources σ is based on the kinematic boundary condition on the wetted part of the lifting surface :

$$\frac{\partial \varphi}{\partial n} = -\bar{V}\bar{n} \quad (6)$$

and on the surface of the ventilating bubble :

$$\frac{\partial \varphi}{\partial t} + U \frac{\partial \varphi}{\partial x} = 0 \quad (7)$$

Both equations refer to a single control point. The lifting surfaces and the free vortex surfaces, similarly as in the case of the lifting line model, are cut by the free water surface which is assumed flat. A mirror image of the vortex/source system must be introduced above the water in order to fulfil the boundary condition on the free water surface. The system fully participates in the calculation of the induced velocity. Within the frame of the linearized theory all vortex/source elements and all control points are located on the surface composed of the mean lines of all blade sections. The number of „active” elements and control points changes with the change of blade immersion during blade revolution. The system of linear equations for the unknown intensity of vortices and sources is formed when the equations (6) and (7) are applied to all active elements in any particular blade position. The system is supplemented by the Kutta condition at the blade trailing edge. After solving the equation system the difference Δp of the pressures on the pressure and suction sides of the blade may be determined on the basis of the Bernoulli equation of a discrete form as follows :

$$\Delta p = -\rho \left[\frac{\Gamma' - \Gamma'^{-1}}{\Delta t} - V_{nab} \sigma_{ab} \frac{\Delta I_q}{\Delta S_{ab}} - V_{iab} (\Gamma_{ab} - \Gamma_{ab-1}) \frac{\Delta I_r}{\Delta S_{ab}} \right] \quad (8)$$

The pressure difference is employed in calculation of the force and moment components of the time-dependent hydrodynamic loading on the blade and also it is used as input data for the structural analysis.

The structural analysis is performed by using the finite element method. The propeller blade is represented within the method as a thick shell composed of 40 eight-node isoparametric elements. According to simplifications typical of thick shells the deformations normal to the element are neglected and both strains parallel to the ele-

ment are assumed constant within the element. This makes using a relatively simple relation between stresses and deformations possible. The analysis leads finally to determination of the normal deformation distribution and reduced stress distribution over the blade.

The above described hydrodynamic and structural analysis is performed in a loop for a number of blade positions covering the submerged part of the propeller disc. The analysis starts with the „vertical down” position in which the intensity of the free vortex system elements is determined. This intensity distribution is assumed to apply to the entire free vortex system throughout the analysis, thus the model is quasi-steady in this sense. Similarly the intensity distribution of vortices and sources determined in this position for the analysed blade applies to the submerged parts of all other blades except for that analysed. Then all prescribed positions of the blade are analysed. In each position new intensities of vortex/source elements are obtained from the boundary condition and then loading distribution, force and moment components, stress and deformation distributions are determined. When this is completed the time-dependent shaft force and moment components are obtained by means of geometric summation of contributions from all blades.

RESULTS OF NUMERICAL ANALYSIS AND COMPARISON WITH EXPERIMENTS

Only selected results of numerical analysis could be compared with the experimental data due to laboratory limitations. Consequently, the following comparisons are presented :

- open water characteristics
- mean values of transverse forces
- time-dependent bending moments on a single blade.

The main parameters of the propeller model are given in Table. Fig.6 shows the comparison of calculated and measured open water characteristics of the surface piercing propeller at the relative submergence of 0.4, 6.6° trim and zero yaw angle. It may be observed that in the vicinity of the design point $J = 1.0$ the numerical calculation produces only small over-estimation of the thrust and a small under-estimation of the torque, which leads to an over-estimation of the propeller efficiency. The serious discrepancies at low advance coefficients are most likely in result of unavoidable simplifications of the theoretical model which does not take into account the strongly dynamic phenomena present during blade entry into the water and blade exit from the water. However despite these differences the general accuracy of numerical prediction of the open water characteristics is not markedly worse than similar predictions for fully submerged propellers and may be considered acceptable. The correlation may be improved by more careful selection of profile drag coefficients which are an empirical correction parameter.

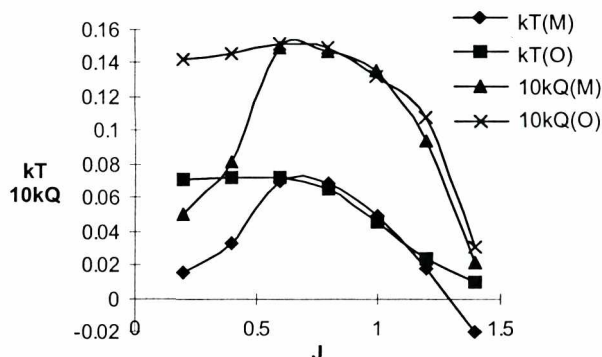


Fig.6. Comparison of measured and calculated open water characteristics of the SPP model (M-measured, O-calculated)

The comparison of measured and calculated mean values of the transverse forces in function of the advance coefficient is presented in Fig.7. This particular example refers to the relative submergence of 0.3, shaft trim angle equal to 12° and shaft yaw angle to +5°. It may be observed that the direction and tendency of changes of both

transverse force components along with the advance coefficient change is quite well reproduced by the calculation. However in the regions distant from the design advance coefficient value the actual values exhibit visible discrepancies with respect to the experimental data. The reason of the discrepancies may be attributed again to the obvious simplifications of the theoretical model.

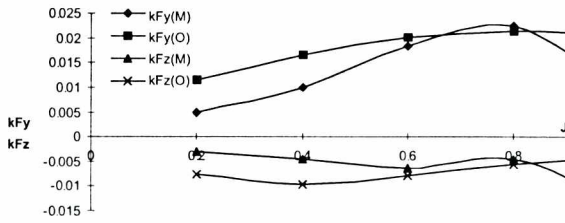


Fig. 7. Comparison of measured and calculated mean transverse forces of the SPP model (M-measured, O-calculated)

Finally a comparison of the calculated and measured time-dependent values of two components of the bending moment on a single blade is presented in Fig. 8 in function of the blade position angle. The presented example refers to the relative submergence of 0.3, shaft trim angle of 6.6° and shaft yaw angle of -5° . The experimental values plotted on this diagram are surprisingly smooth, especially no evidence of high impact forces is visible in the region of blade entry into the water. The calculated values reproduce reasonably well the maxima of both bending moments, although locally the discrepancies are quite substantial. In particular the theoretical model was unable to predict correctly the regions of the blade entry to and blade exit from the water.

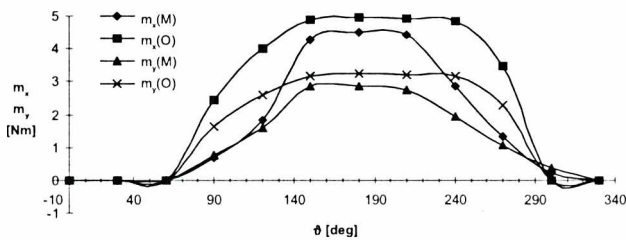


Fig. 8. Comparison of measured and calculated time-dependent bending moments on the blade of the SPP model (M-measured, O-calculated)

The scope of the experiments did not include measurements of blade stress and blade deformation distributions, therefore the results of numerical structural analysis could not be directly compared with the experimental data.

CONCLUSIONS

The following conclusions may be drawn from the presented description of the theoretical models and comparisons of the calculation and experimental results :

- both theoretical models : for design and for analysis take into account the presence of free water surface cutting through the blades, the main feature differing surface piercing propellers from ordinary submerged propellers
- the presented theory neglects important dynamic effects connected with blade impact against the water and, in particular, that the real free surface in the vicinity of the working propeller is far from flat
- the theoretical models are able, despite numerous simplifications, to provide the results in reasonable agreement with the experimental data especially for the conditions in the vicinity of the design point
- both the design and analysis procedures may be employed for development of surface piercing propellers but further experimental verification and improvement of the theoretical models is necessary.

Acknowledgment

The experimental and theoretical research presented in this paper was performed within the research project PB071/T12/96/11 funded by the State Committee for Scientific Research and conducted in the Institute of Fluid Flow Machinery of the Polish Academy of Sciences.

Special thanks are due to the staff of the model basin of CTO for preparation and conducting of the model experiments.

NOMENCLATURE

- a, b - indices locating point on the lifting surface
 c_L - lift coefficient
 c_D - drag coefficient
 f - maximum mean line camber
 F_x - axial force on a single blade
 ΔI_Q - source element
 ΔI_r - vortex element
 J - advance coefficient
 k - non-dimensional force coefficient
 k_T - thrust coefficient
 m_x, m_y - components of the bending moment on a single blade
 \bar{n} - local normal vector
 Δp - pressure difference across the blade
 r - non-dimensional radius
 r_i - starting point of the submerged part of the blade
 ΔS_{ab} - blade area element
 t - time
 T - propeller thrust
 Q - propeller torque
 U - local inflow velocity (sum of advance and rotation components)
 V - ship speed
 V_n - normal component of velocity
 V_t - tangential component of velocity
 β - advance angle
 β_i - induced advance angle
 φ - velocity potential
 Γ - vorticity
 ϑ - blade position angle
 ϑ_1 - position angle of blade entry into the water
 ϑ_2 - position angle of blade exit from the water
 ρ - water density
 σ - source intensity

BIBLIOGRAPHY

1. Furuya O.: „A Performance Prediction Theory for Partially Submerged Ventilated Propellers”. Proceedings of 15th Symp. on Naval Hydrodynamics. September 1984
2. Miller W., Szantyr J.: „Model Experiments with Surface Piercing Propellers”. Paper presented at HYDRONAV'97, Szklarska Poręba, September 1997
3. Sanchez-Caja A.: „Partially Submerged Propellers on Large Fast Ships - An Analysis Theory”. Proceedings of FAST'97, Sydney, July 1997
4. Szantyr J.: „Experimental Study of Surface Piercing Propellers for a Patrol Boat”. Proceedings of FAST'97, Sydney, July 1997
5. Szantyr J.: „Theoretical Model of a Surface Piercing Propeller” (in Polish). Report of the Institute of Fluid Flow Machinery No.465/96. Gdańsk 1996
6. Oloffson N.: „Force and Flow Characteristics of a Partially Submerged Propeller”. PhD Thesis. Chalmers University of Technology. Gothenburg 1996
7. Vorus W.S.: „Forces on Surface Piercing Propellers with Inclination”. Journal of Ship Research, September 1991, Vol.35, No. 3

